INL REPORT

INL/EXT-16-40023
Unlimited Release
Printed September 2016

Analysis Methods and Validation Activities for MAMMOTH Using M8 Calibration Series Data

Benjamin A. Baker, Javier Ortensi, Mark D. DeHart, Yaqi Wang,
Sebastian Schunert and Frederick N. Gleicher

Prepared by
Idaho National Laboratory
Idaho Falls, Idaho 83415

The Idaho National Laboratory is a multiprogram laboratory operated by
Battelle Energy Alliance for the United States Department of Energy
under DOE Idaho Operations Office. Contract DE-AC07-05ID14517.

Issued by the Idaho National Laboratory, operated for the United States Department of Energy by Battelle Energy Alliance.

INL/EXT-16-40023
Unlimited Release
Printed September 2016

Analysis Methods and Validation Activities for MAMMOTH Using M8 Calibration Series Data

Benjamin A. Baker, Javier Ortensi, Mark D. DeHart, Yaqi Wang,
Sebastian Schunert and Frederick N. Gleicher

Reactor Design and Analysis Department
Idaho National Laboratory
2525 Fremont St
Idaho Falls, ID 83415

Executive Summary

This report provides a summary of the progress made towards validating the multi-physics reactor analysis application MAMMOTH using data from measurements performed at the Transient Reactor Test facility, TREAT. The work completed consists of a series of comparisons of TREAT element types (standard and control rod assemblies) in small geometries as well as slotted mini-cores to reference Monte Carlo simulations to ascertain the accuracy of cross section preparation techniques. After the successful completion of these smaller problems, a full core model of the half slotted core used in the M8 Calibration series was assembled. Full core MAMMOTH simulations were compared to Serpent reference calculations to assess the cross section preparation process for this larger configuration. As part of the validation process the M8 Calibration series included a steady state wire irradiation experiment and coupling factors for the experiment region. The shape of the power distribution obtained from the MAMMOTH simulation shows excellent agreement with the experiment. Larger differences were encountered in the calculation of the coupling factors, but there is also great uncertainty on how the experimental values were obtained. Future work will focus on resolving some of these differences.

Contents

1 Introduction 1
2 Methods 3
3 Cross Section Development 5
3.1 Description of Diffusion Coefficient Options 5
3.2 Standard Element 6
3.3 Slotted Elements 7
3.4 Control Rod Element 8
3.5 Experiment Location 9
3.6 Full Core (Rod Configuration A) 11
3.7 Best Practices 12
4 Results 13
4.1 M8 Experiment Power Profile 13
4.2 M8 Power Coupling Factors 13
5 Conclusions 19
Appendices 19

Figures

1 Slotted Element 3x3 Core 7
2 Control rod 3x3 supercell (x-y plane, left) and (y-z plane, right) 9
3 5x5 model with the M8CAL experiment location 10
4 Axial power profile comparisons with full-length flux monitor wires 14
5 Calculated Experiment Power Profile with Serpent and MAMMOTH 14

Tables

1 TDC Angular Convergence Study with a G-C Quadrature Set 10
2 TDC Angular Convergence Study with a L-S Quadrature Set 11
3 Values from Simulations 15
4 M8CAL Lower-Level Steady State Flux Monitor Wire Coupling Factors 16
5 Coupling Factors Comparisons [fissions/g U-235-MJ x 10^{12}] 16

Acronyms

ATF	Accident Tolerant Fuels
DOE	Department of Energy
G-S	Gauss-Chebyshev
INL	Idaho National Laboratory
L-S	Level-Symmetric
M&S	Modeling and Simulation
M8CAL	M8 Calibration Series
PCF	Power Coupling Factor
RMS	Root Mean Square
SPH	Super-Homogenization
TDC	Tensor Diffusion Coefficients
TREAT	Transient REActor Test Facility

1 Introduction

The Transient Reactor Test Facility (TREAT) was constructed and began operation in 1959 and operated for 35 years until it was placed in a standby state in 1994. TREAT is in the process of being brought back to operational readiness to resume transient testing, beginning with the accident tolerant fuel (ATF) campaign in 2018. Because of the greater than 20 year time span since initiation of standby status, the computational power and simulation capabilities have increased substantially since TREAT last operated and allow for new modeling possibilities that were not practical or feasible for most of TREATs operational history. This provides a unique opportunity to apply state-of-the-art software and associated methods in the modeling and simulation (M&S) of general 3-D kinetic behavior for reactor operation and coupling of the core power transient model to experiments.

The MAMMOTH [1] reactor multi-physics analysis application is being developed as the primary tool for M&S of TREAT. MAMMOTH was developed using the MOOSE framework [2, 3], a finite element method development environment that focuses on multi-physics simulations with strong or tight coupled physics applications. Some of the benefits of MOOSE are parallel processing for large problems, one, two and three-dimensional finite element modeling support and a coherent code development environment such that any code developed by other developers will share a common framework and cand be linked to one another (shared data) within that framework. Thus, it is possible for independent physics codes to be applied as needed without special external code development to provide physics coupling. MAMMOTH is in fact a control application that inherently and seamlessly interfaces with several other MOOSE applications including Rattlesnake [4] for solving the Boltzmann transport equation, BISON [5, 6] for heat transfer and fuel performance modeling and RELAP-7 [7] for thermal fluids calculations. MAMMOTH itself provides both macro- and micro-depletion capabilities [8]. Several preliminary studies of TREAT have already been conducted with MAMMOTH [9, 10] .

In order to perform a MAMMOTH calculation, the most basic required components are a mesh for the finite element solution, and cross section data, which define the transport material properties for the finite elements.

For the work provided here, efforts are described for the process of validation of MAMMOTH using data from the most recent calibration experiments performed in the core, the M8 calibration series (M8CAL) [11]. The majority of the work performed to-date centers around cross section preparation to get representative cross sections for the core. Initial work began with the full core model, which yielded unusual results that could not be identified. It was decided to go down to basic configurations to better understand cross section development issues. The geometry was kept as simple as possible with the limitation that the mesh was axially extruded so that all of the elements share the same axial discretization. Therefore, materials (cross section regions) were allowed to vary axially within a physical TREAT element, but were radially homogenized within the physical element.

2 Methods

The Serpent 2 [12] Monte Carlo code is used to prepare spatially-homogenized and energy-condensed cross sections and to generate reference results. One of the great advantages is that Serpent allows the preparation of cross sections from full core geometries, thus including 3-D effects that are difficult to treat in traditional 2-D lattice physics calculations.

Some regions of the TREAT core allow neutrons to stream freely without interacting with matter. The presence of these streaming regions adversely affects the diffusion calculation since air/void regions are outside the range of applicability of diffusion theory (note that these streaming regions are also a challenge to higher order transport methods). Appropriately corrected scalar diffusion coefficients can improve the average flux values within these streaming regions, but this can be to the detriment of neighboring regions if the flux is severely anisotropic (such as near stong absorbers, e.g., control rods). In this case, appropriately corrected anisotropic diffusion coefficients are needed to overcome the limitations of diffusion theory. Weighted diffusion coefficients can be provided in either scalar, vector or tensor form.

The magnitude of the scalar diffusion coefficient produced directly from Serpent, with the current methodology, can be on the order of hundreds to thousands of cm in or near streaming regions, which will dominate the diffusion equation and produce incorrect results. In order to close this gap, a Larson-Trahan methodology [13] was added to Rattlesnake [14]. This method allows the determination of tensor-based diffusion coefficients, or TDCs, using the S_N transport solver within Rattlesnake.

The Super-Homogenization (SPH) method [15, 16] is an equivalence technique used to preserve reference reaction rates by adjusting cross sections in designated constant material regions. This process attempts to correct/minimize the error introduced by the spatial-homogenization and energy-condensation of the cross sections.

These techniques and their use in TREAT calculations are described in [14, 16] and are not discussed in detail here. However, this work demonstates the relative value of each type of approach and provides best-practices recommendation for employing these methods in TREAT simulations.

3 Cross Section Development

The typical steps taken for the development of the cross sections [14] consist of:

1. Perform a Monte Carlo simulation using the Serpent code to prepare cross sections,
2. Run a Rattlesnake calculation to develop a set of TDCs for neutron streaming regions, and
3. Perform an SPH calculation to correct for the error introduced in the homogenization and condensation processes.

A series of simple geometries were studied such that the effects of a single type of TREAT element could be explored, before moving to smaller mixed element cores and ultimately a full core. This fundamental step allows for a better understanding of the cross sections and methods required to perform high fidelity simulations of TREAT. Each section below summarizes the work performed and the lessons learned.

3.1 Description of Diffusion Coefficient Options

There are various options/sources from which the diffusion coefficients can be obtained and are listed below. In addition to the generation of the diffusion coefficients, there are three representation options available in Rattlesnake: scalar, vector and tensor. A given cross section library file may contain a mixture of all types. The user has the option to specifying which form to use, thus letting Rattlesnake either reduce or expand the diffusion coefficients into the desired form. The default form is the scalar form.

The following list describes the nomenclature used in this report to describe the generation of diffusion coefficients for Rattlesnake:

1. *Generic* The cross sections obtained directly from a Serpent calculation that includes diffusion coefficients. These diffusion coefficients are in scalar form.
2. *Local* Uses the Serpent-calculated total and scattering cross sections to calculate diffusion coefficients. These diffusion coefficients are also in scalar form.
3. *Point-wise TDC* Diffusion coefficients generated from a TDC calculation which preserve the point-wise values from the transport solution. The data must be passed from one application to another via the MOOSE Transfer system. The diffusion coefficients are in tensor form.
4. *Region-wise TDC* Diffusion coefficients generated from a TDC calculation that has been averaged over a spatial material region and saved in a cross section data file. These diffusion coefficients are also in tensor form.

3.2 Standard Element

A 3x3 element model with all standard TREAT fuel elements was generated. This model was used to perform a mesh convergence study, to test the TDC and SPH methods and other possible options, such as using the local diffusion coefficients or point-wise TDCs. The metrics used to compare the results included comparison of the eigenvalue, source rate, absorption rate, leakage rate, flux and power distribution in the active core region. Because reflective boundary conditions were used on x and y boundaries, the core is infinite on the (x,y) plane. Vacuum boundary conditions were applied on the z boundaries, above and below the axial reflector regions. Hence the active core consists of an infinite lattice of 121.92 cm (4 ft) tall fuel regions.

The mesh convergence study used a base mesh with elements of ~10 cm in height. The studies involved increasing the uniform refinement option available within MOOSE from 0-2 (the number indicates the number of uniform mesh refinements from the base mesh). The results showed that the eigenvalue changed by ~19 pcm between the uniform refine 0 and 1 option. The difference between the uniform refine 1 and 2 option was ~4 pcm and was considered to have been converged with the use of uniform refine 1, which corresponded to an element height of ~5 cm.

Various studies were performed to examine the percent error in the eigenvalue, source rate, absorption rate, leakage rate, flux and power. These studies were further subdivided into diffusion coefficient development and cross section corrections using SPH.

The three diffusion coefficient methodologies beyond the generic Serpent coefficients, described in Section 2, were investigated. The differences in the results between the point-wise and region-wise TDCs were not significant, and the simpler region-wise method of generating cross sections was employed in the remainder of the calculations described in this report. The tensor and scalar options were the only options explored.

The TDC results were found to increase the eigenvalue error relative to the reference solution by ~700 pcm, with or without the application of SPH. The result was worse compared to the equivalent path without the TDC calculation. Note that this is only for the standard element, where standard diffusion approaches should work well. The results are consistent with theory, since Larson-Trahan TDCs should only be applied to optically thin media. Applying the *local* diffusion coefficient marginally improved the result by ~200 pcm for both the cross sections coming directly from Serpent and those after the SPH calculation. The tensor/scalar variation was not applied to all cases and were only applied to the TDC cases, where a difference of ~200 pcm was obtained, with the scalar treatment providing the better solution relative to the tensor treatment.

SPH was the main means for obtaining good results and was marginally improved by using the *local* option for diffusion coefficients. The difference in the eigenvalue was 407 pcm with SPH applied directly to the generic cross sections and 220 pcm with the local diffusion coefficients and SPH. The errors in the power distribution were on the order of -0.6 to 0.28 % for SPH only and -0.28 to 0.16 % for SPH with the local option diffusion correction added.

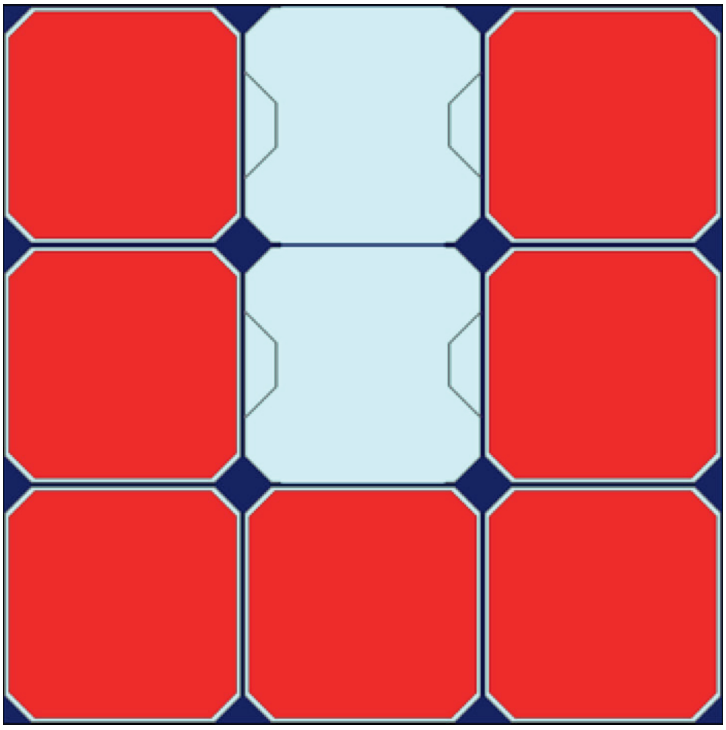

Figure 1: Slotted Element 3x3 Core

3.3 Slotted Elements

The slotted element test involved a radially reflected 3x3 supercell, depicted in Fig. 1, with the center and top-middle elements replaced with slotted elements, while the remainder of the elements were standard elements. Similar tests to those discussed in Section 3.2 were conducted. A 5 cm height axial mesh was used, but no additional mesh refinement study was performed.

It was expected that the slotted element tests would perform much better with the introduction of TDCs than had been found in the standard element studies. However, initial tests showed similar behavior to that encountered in the standard elements. These results were later attributed to applying the diffusion coefficients obtained from the TDC calculation to the entire 3x3 core, which had an adverse effect on the standard elements. Better results were obtained by applying TDCs only to those zones with large air/void regions (i.e., within the slotted elements). The TDC calculations used both a Level-Symmetric (L-S) S_{12} quadrature set and a Gauss-Chebyshev (G-C) quadrature set with 12 polar angles and 2 azimuthal angles with similar results.

When comparing the percentage differences from the various metrics, it was not clear which methods were the best for the slotted elements. Many of the metric values were similar for various methods or there was a trade-off that had to be made, and the question became which metric was most important. For instance, the power distribution was considered to be the most important because the power is the source term for a transient, while the leakage rate was allowed to have more error since it is a smaller fraction of the balance equation.

Unlike the standard element core, the slotted element studies included more calculations showing the difference between the tensor/scalar options. There was not a clear indication that one was better than another. The practice has since been to select one approach and continue to use it for all subsequent calculations.

The best results obtained for the eigenvalue came from the SPH-corrected cross sections and the local option for the diffusion coefficients, with an error of 259 pcm. However, as mentioned above, the most important metric should be the power distribution. This result had min/max errors of -2.2 to 2.8% with an RMS of 1.16%, while the best result for the power distribution came from the SPH calculation using the TDC values applied only to the air portions of the slotted elements. The value was -0.6 to 0.4%, with an RMS of 0.191% error in power. The eigenvalue, on the other hand, was 858 pcm off because of a larger error in leakage rate.

The slotted element studies lead to the conclusion that it is best to apply the TDC diffusion coefficient to regions where there is a large amount of air present, but there is no clear method for obtaining the best results. It was decided that the path forward would be to use the TDC diffusion coefficients applied to the air regions followed by SPH.

3.4 Control Rod Element

The control rod element studies involved a 3x3 supercell with the control rod in the central position and the bottom of the borated region of the control rod located near the axial midpoint of the active core region. This position was chosen because it is the region of greatest neutron importance. The other elements in the 3x3 lattice were comprised of the standard elements. Similar studies were performed as those described in Sections 3.2 and 3.3.

The power distribution comparisons between MAMMOTH and Serpent models for the controlled supercell indicated the presence of major discrepancies regardless of the method. These initial differences were attributed to a deficiency in the number of axial spatial cross sections regions necessary in order to model a partially inserted rod. As shown in Fig. 2, the control rod is partially inserted in a large cross section region, where flux-averaged cross sections are prepared. This will lead to poor cross sections, since the fluxes below and above the control rod are very different.

In order to remedy these large differences in the power distribution, extra axial regions were added, including two 5 cm regions immediately above and below the boron interface. It was believed that since boron is a large neutron absorber and graphite has a large migration length, the effects from the boron can be felt for some distance away from the actual boron location. Adding extra axial regions would help to limit the errors caused by the strong absorber.

After implementing the extra axial cuts/cross section regions, a limited number of tests were performed due to time constraints; this will be investigated further in continuing work. The TDC calculations seemed to have no particular advantage, as was noted with the standard elements, and the local option was used to generate the diffusion coefficients. After SPH was applied, the eigenvalue was 176 pcm in error, and the power profile had a min/max error of -2.7 to 4.0% on the

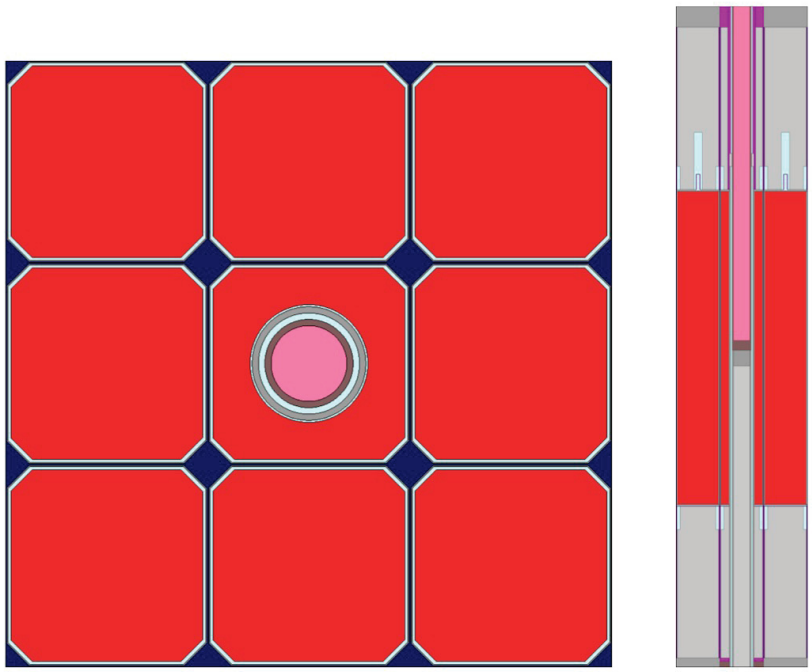

Figure 2: Control rod 3x3 supercell (x-y plane, left) and (y-z plane, right)

control rod and -2.8 to 1.5% for the neighboring standard elements. The average for the entire 3x3 core power distribution was -2.7 to 1.4% error.

3.5 Experiment Location

A 5x5 model, shown in Fig. 3, was developed which had a simplified M8CAL vehicle in the center, with a half-dummy graphite element on the south side and a half-slotted element to the north side (as exist in the actual core), followed by regular slotted elements. The balance of the supercell consisted of standard elements. The experiment tube was filled with a material equivalent to the L91-60-1 flux wire used in M8CAL measurements [11]. The actual flux wire was much smaller than the tube, but in an effort to improve the reaction statistics during the Serpent cross section development, the atom ratios were modified to maintain the same mass but increase the volume.

The practice of using TDCs exclusively in the air/void regions was well-established by the time the experiment vessel was evaluated. The major problem with the TDC calculation is the fact that it requires a transport calculation, which is much slower and uses more memory than diffusion. An angular convergence study was performed to determine the sensitivity on the diffusion coefficients to the angular discretization. Both L-S and G-C quadrature sets with varying angular values were used in the study.

The metrics for comparison consisted of looking at the error in the power for the element to the

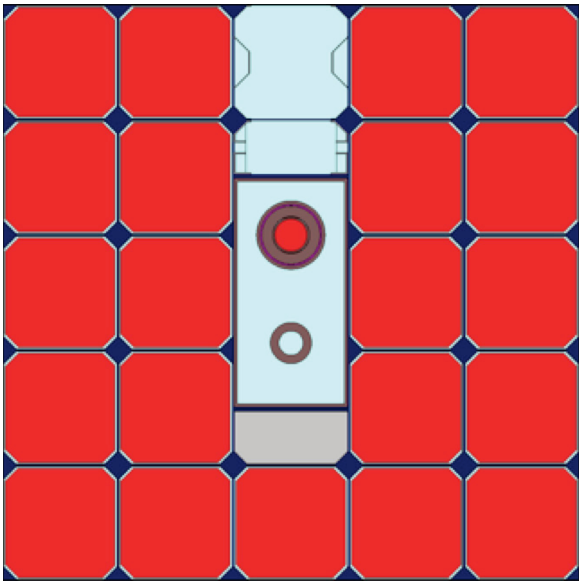

Figure 3: 5x5 model with the M8CAL experiment location

Table 1: TDC Angular Convergence Study with a G-C Quadrature Set

Polar Angles	Azimuthal Angles	Position (2,2) Range %Error	Experiment Range %Error
2	2	3.097	6.949
4	2	2.299	7.004
6	2	2.123	7.025
12	2	2.179	7.201
4	4	1.989	7.300
6	6	1.850	7.404

corner of the experiment by the half-slotted element at location (2,2) and the experiment itself, located at (3,3). The results for the TDC-SPH calculations are shown in Table 1, and Table 2. The figure of merit in the comparisons is the range (maximum minimum values) in the difference versus the reference calculation.

From the table it can be seen that results with 12 polar and 2 azimuthal angles were identical to S_{12} quadrature. There is a clear increase in difference for the standard element as the number of Level-Symmetric angles decreases. However, this increase in error is not as evident in the Gauss-Chebyshev results until the number of polar angles drops to 2. The increase in the azimuthal angles seems to have marginal benefit for the standard elements but adversely affects the experiment region. These results prove that the diffusion coefficient is weakly dependent on the higher order angles and it is left up to the user to determine the desired fidelity for the TDC calculation while keeping in mind the added cost for such a calculation.

Table 2: TDC Angular Convergence Study with a L-S Quadrature Set

Level-Symmetric	Position (2,2) Range %Error	Experiment Range %Error
S_4	3.839	6.889
S_6	3.009	6.933
S_8	2.521	7.014
S_{12}	2.179	7.201

3.6 Full Core (Rod Configuration A)

The full core model is based on the M8 Calibration core with a half-slotted element and the control rods located in the A configuration [11], which has the control/shutdown rods nearly banked at 55.88 cm (22 inches) and the compensation and transient rods fully withdrawn.

In the earlier studies, the geometry was small enough to allow the development of cross sections for each individual element within Serpent (known as the *block ID* within MAMMOTH). With the full core configuration the grouping of similar TREAT elements is introduced to limit the memory usage and run-time of the calculation. However, this approach inserts a new variable, and more uncertainty, in the calculation of cross sections. There is no simple methodology to determine the optimal grouping of cross section regions at this time. The two traditional approaches involve engineering judgment based on geometry and physics and a full determination of spectral regions and grouping of similar spectral regions for the same material.

A few models were constructed with varying number of grouped physical element regions, which are designated with block IDs in the MAMMOTH inputs. Two configurations of interest had 83 and 37 block IDs. A TDC calculation was not practical with the 83 block ID core model, due to memory requirements, therefore diffusion coefficients were obtained from the 5x5 model described in Section 3.5. The 83 block ID core showed signs of poor statistical values for the cross section in the highest energy group and a test was performed using 10 energy groups instead of 11 (collapsing the top two energy groups into a single energy range. The original 11 group structure had errors for the full core power profile in the range of -2.8 to 5.7% with RMS=0.513% and $\pm$ 4% on the experiment values. The 10 group structure had errors for the full core of -3.7 to 5.8% with RMS=0.882% and -6 to 4% for the experiment values. The 37 block ID model was also analyzed using 10 energy groups and was found to have error for the full core power profile within the range of -6.2 to 5.4% with RMS=1.15% and -4.8 to 2.9% for the experiment values.

Any of these cores could be considered acceptable depending on the tolerance that is desired. The best indicator for the full core results is the RMS value (the root mean square of the errors for all elements) since it gives a value that is applicable to the whole core and not just the extreme values.

3.7 Best Practices

Based on the series of single assembly, slotted core and full core studies, the following set of guidelines were determined to be the best practices in the cross section development process.

1. Use TDC cross sections in optically thin media.
2. Apply the *local* option for optically thick media.
3. Stay consistent in the usage of the scalar and tensor kernel option for a series of calculations.
4. Add axial regions to reduce the error near the boron region in the control rod axial interface.

4 Results

The results from the full core models are discussed in this section. Two experimental comparisons are undertaken. Section 4.1 covers the results from a comparison to the power distribution obtained with a flux wire in the M8 experiment location. Section 4.2 deals with the calculation of the coupling factor for various M8 steady state irradiations.

4.1 M8 Experiment Power Profile

As part of the M8 Calibration series, a power profile was experimentally determined using the L91-60-1 flux wire with the rods near the A configuration [12]. The data supplied in the M8CAL report is normalized so the peak value is one, so the same normalization is applied here.

In the previous section, errors were presented for comparison between the Serpent and MAMMOTH calculations for the full core and the experiment power profile. It should be mentioned that the Serpent detectors (i.e., tallies) provide the total power for a region and are compared to the MAMMOTH calculation by multiplying the volume by the power density of the MAMMOTH calculations. The total power, rather than power density, is the best metric to compare the accuracy between the two codes since MAMMOTH relies on a homogenized region and the experiment zone is effectively larger in MAMMOTH than the Serpent counterpart.

The computed powers are used to generate the relative shape of the power profile. Figure 4 is included to provide the means of comparison of the Serpent and MAMMOTH calculations against measured data [12]. The original data is available only in the form of a plot [11]. Similar scaling is used to aid in comparisons. Further, there are fewer data points in the calculations because they were only obtained between mesh points. The data presented from MAMMOTH and Serpent is from the full core configuration using 83 block IDs. The result does not change significantly with other configurations.

Figure 4 shows the axial power profile for the M8CAL measurements, indicated with black triangles, along with the M2 calibration data that was also provided on that plot, indicated with white squares. Figure 5 shows the Serpent and MAMMOTH calculated results. The results for the shape obtained with MAMMOTH show excellent agreement. In addition, the values from both simulations are provided in Table 3. The root-mean-square value of the relative difference in the power distribution was 2.7% with a maximum and minimum values of 2.6% and -5.4%, respectively.

4.2 M8 Power Coupling Factors

The power coupling factor (PCF) is a unit that has been used in TREATs history to help predict the amount of energy deposited in the experiment. The units for a power coupling factor are fissions/g-U235 (in the experiment) per MJ of energy in the full core. It was assumed that the coupling factor only applies to the peak location for the flux wire/fuel pin instead of the integral over the entire

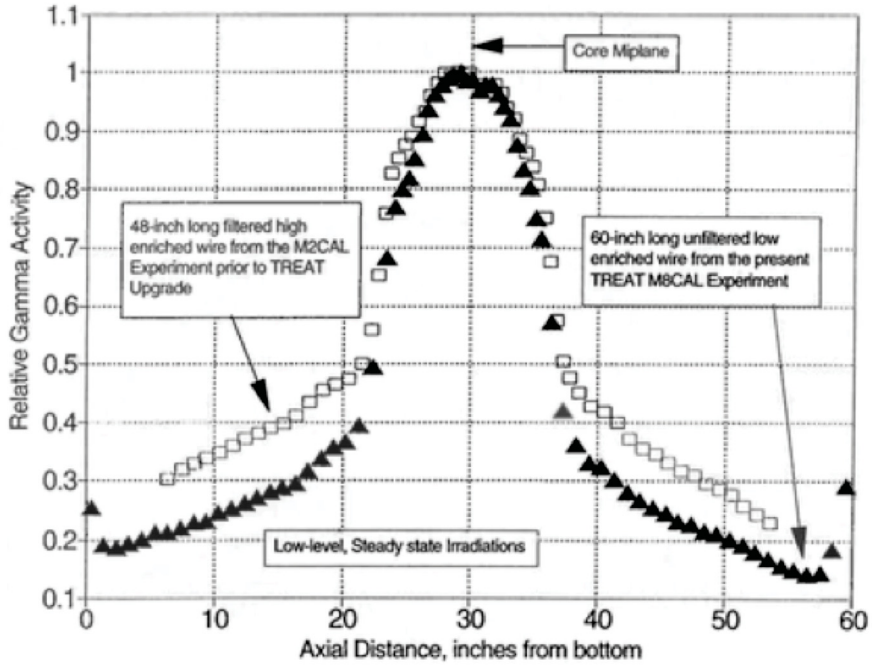

Figure 4: Axial power profile comparisons with full-length flux monitor wires

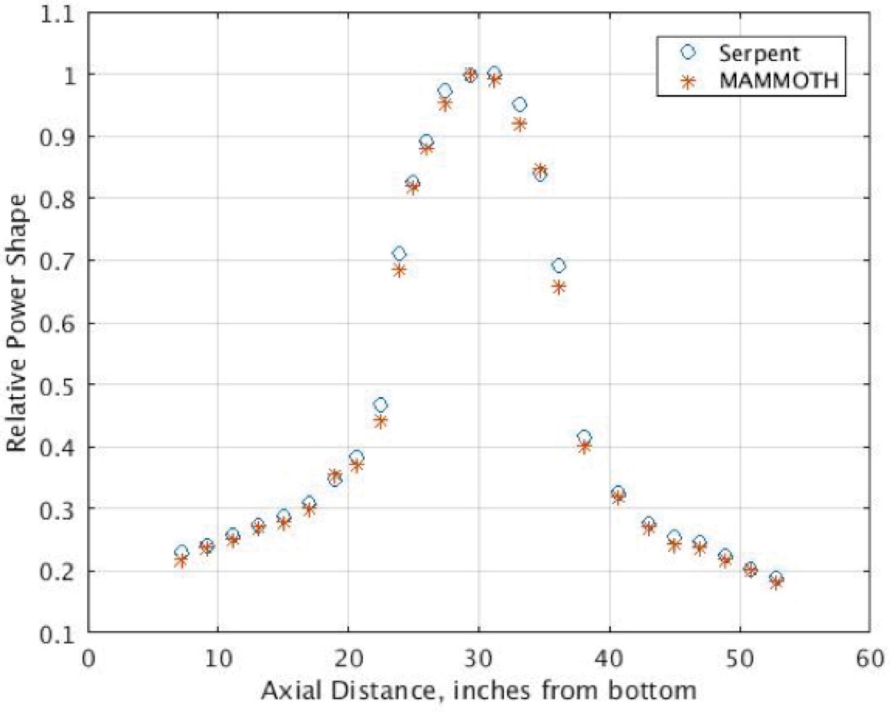

Figure 5: Calculated Experiment Power Profile with Serpent and MAMMOTH

Table 3: Values from Simulations

Position (inch)	Serpent	MAMMOTH
7.172	0.230	0.220
9.140	0.242	0.237
11.109	0.257	0.253
13.077	0.272	0.271
15.046	0.286	0.278
17.015	0.310	0.302
18.875	0.346	0.355
20.625	0.384	0.373
22.375	0.467	0.442
23.831	0.712	0.686
24.934	0.825	0.821
25.978	0.892	0.880
27.438	0.973	0.953
29.313	0.998	1.000
31.188	1.000	0.991
33.063	0.952	0.922
34.688	0.840	0.848
36.063	0.693	0.658
38.063	0.416	0.403
40.688	0.325	0.321
42.985	0.277	0.272
44.954	0.253	0.243
46.923	0.246	0.238
48.891	0.224	0.219
50.860	0.202	0.202
52.828	0.189	0.184

wire based on information provided in the M8 Calibration report. Note that this assumption may be revised as more information becomes available on the experiment, or it may be possible there are multiple interpretations depending on the desired application.

The first value for the PCF was determined for the L91-60-1 flux wire with the full core model. This particular coupling factor is for a steady state irradiation, and simulations use the ratio of powers instead of energy deposited. Since the power for the experiment can be expressed in terms of fissions/second and the power for the core is in MJ/second, the *seconds* terms will cancel. The PCF was determined for the simulations by converting the total power for a volume to fissions/second, dividing by the mass inside of this volume and then dividing by the full core power in MW. Note that the default energy per fission heating value in Serpent and consequently in MAMMOTH is 202.27 MeV/fission. Even though the heating value is of no consequence in this case, since the final result is divided by the entire core power, it will play an important role in the determination of transient coupling coefficients.

The result obtained for the L91-60-1 flux wire was 1.19E+12 f/(g U-235-MJ) for Serpent and 1.21E+12 f/(g U-235-MJ) for MAMMOTH. The experimentally determined value was 1.40E+12 f/(g U-235-MJ) which is 15% higher than the calculated value. It is significant to note that the prediction from MAMMOTH is within 1.68% of the Serpent value.

A short study was initiated to determine if other coupling factors for the steady state irradiations in the M8 Calibration series could be predicted with the Serpent model. Data from the Ref. [11] is included in Table 4, and it shows the changes made to the core between the flux wire irradiations. The naming convention for the flux wires is e91-l-n where e is L for low enriched and H for high enriched, l is the length in inches of the flux wire and n is the wire number in the series. Flux wires L91-60-1, L91-8-1 and L91-8-6 are nearly identical configurations, with the only difference being the length of the flux wire.

Table 4: M8CAL Lower-Level Steady State Flux Monitor Wire Coupling Factors

Item	Date	Wire Identification	Core Slot	Axial Peak: Absolute (f/g) (x10E13)	Total Energy in Irradiation, MJ	Measured Coupling Factor (f/g U-235-MJ) (x10E12)	Control Rod Configuration	Appropximate Initial (Critical) Rod Position, in.		Wire Holder
								Control/Shutdown	Transient	
1	10/19/90	L91-8-10	Full	1.42	667	1.79	B	Fully Withdrawn	18.5	Unfiltered
2	8/24/92	L91-60-1	Half	0.958	576	1.40	A	22	Fully Withdrawn	Unfiltered
3	11/20/92	L91-8-1	Half	0.968	576	1.41	A	22	Fully Withdrawn	Unfiltered
4	2/ 8/93	L91-8-6	Half	0.819	480	1.44	A	22	Fully Withdrawn	Unfiltered
5	2/12/93	H91-8-1	Half	0.972	576	0.503	A	22	Fully Withdrawn	Filtered
6	3/ 2/93	L91-8-16	Half	1.26	576	1.84	B	48	11.5	Unfiltered

The results obtained with the Serpent model are shown in Table 5. The calculation for item number 3a was repeated because the M8CAL report appears to indicate that there was an additional filter for the high-enriched flux wire due to potential melting problems. The report seems to indicate that the 20-mil thick dysprosium collar was placed around the center. There is a reference to a drawing number, but to date the drawing has not been located.

Table 5: Coupling Factors Comparisons [fissions/g U-235-MJ x 10^{12}]

Item	Wire	Measured	Predicted	% Error
1	L91-8-10	1.79	1.204	-32.7
2	L91-60-1	1.40	1.19	-15.0
3a	H91-8-1	0.503	1.26	150.5*
3b	H91-8-1 (Filter Added)	0.503	0.439	-12.7
4	L91-8-16	1.84	1.24	-32.6

* Dysprosium filter not present in model

The power coupling factor values calculated are reasonable for items 2 and 3b. However, during the course of the analysis it was determined that the coupling factors from Serpent did not change

significantly even though the core was drastically changed with the slotted elements or control rod positions. The value remained 1.2E+12 for all cases except for item 3b where an extra dysprosium collar was added. This suggests that the method of determining the coupling factors might be incorrect, since there appears to be a systematic error when analyzing the data from Serpent or there is a problem in modeling the core, which is less likely. As mentioned in the beginning of this section, it is believed that the coupling factor is based on the peak value. If the integral were taken over the whole flux wire, then the result from Serpent would be even lower because the flux wires have a uniform density of U-235, thus the integral number of fissions/gram would be less than at the peak which would make the results worse.

5 Conclusions

A series of calculations were performed to assess the best calculation sequence to prepare cross section to analyze the M8 calibration core configuration. The series included models with standard, control rod, and slotted TREAT elements, as well as the M8 experiment vehicle. During this process, it was found that the TDC calculation for diffusion coefficients should be applied exclusively to regions that contain large amounts of air/void, since its use had a negative impact on optically thick media. The only exception was the top axial region in the full core simulation where the void boundary condition is imposed and the Serpent calculation has poor statistics due to the reduced flux (and perhaps also influenced by Serpent's use of *delta tracking*.[17] This will be investigated in future work. However, these studies showed that using the local option in MAMMOTH, which calculated the diffusion coefficients using the total and scattering cross sections, worked well for optically thick media. In all cases, the SPH calculation significantly improved the results.

The L91-60-1 power profile from the M8 Calibration series appears to be in good agreement with the MAMMOTH calculation. The coupling factor predicted with MAMMOTH is 1.68% higher than the Serpent reference. Therefore, the MAMMOTH deterministic model can predict accurately the coupling factor from cross sections obtained from the Monte Carlo simulation. Other coupling factors were calculated with Serpent for various M8CAL configurations. Two of the configurations produced results that were within an acceptable range. However, most of the results seemed to be invariant to the changes in the reactor system, which indicates something imay be incorrect in the calculation of coupling factors. Future work will also focus on determination of the reason for the discrepancy.

References

[1] F.N. Gleicher and J. Ortensi et al. The Coupling of the Neutron Transport Application Rattlesnake to the Fuels Performance Application BISON. In *International Conference on Reactor Physics (PHYSOR 2014)*, Kyoto, Japan, May 2014.

[2] R&D Magazine. 2014 R&D 100 Award Winners. "http://www.rdmag.com/award-winners/2014/08/2014-r-d-100-award-winners.

[3] D. Gaston, C. Newman, G. Hansen, and D. Lebrun-Grand'e. MOOSE: A parallel computational framework for coupled systems of non-linear equations. *Nucl. Eng. Design*, 239(1768-1778), 2009.

[4] Y. Wang. Nonlinear Diffusion Acceleration for the Multigroup Transport Equation Discretized with SN and Continuous FEM With Rattlesnake. In *Proceedings of the International Conference on Mathematics, Computational Methods & Reactor Physics (M&C 2013)*, Sun Valley, Idaho, USA, ID, May 2016.

[5] R.L. Williamson et al. Multidimensional Multi-physics Simulation of Nuclear Fuel Behavior. *Jou. Nucl. Mat.*, 423(149–163), 2012.

[6] J. D. Hales et al. Advanced multiphysics coupling for lwr fuel performance analysis. *Annals of Nuclear Energy*, 84:98–110, 2015.

[7] D. Andrs et al. RELAP-7 Level 2 Milestone Report: Demonstration of a Steady State Single Phase PWR Simulation with RELAP-7. Technical Report INL/EXT-12-25924, Idaho National Laboratory, 2012.

[8] J. Ortensi et al. Initial Testing of the Microscopic Depletion Implementation in the MAMMOTH Reactor Physics Application. Technical Report INL/EXT-16-39930, Idaho National Laboratory, Idaho Falls, ID, Sept. 2016.

[9] J. Ortensi, M. D. DeHart, F. N. Gleicher, Y. Wang, S. Schunert, A. L. Alberti, T. S. Palmer. Full Core TREAT Kinetics Demonstration Using Rattlesnake/BISON Coupling Within MAMMOTH. Technical Report INL/EXT-15-36268, Idaho National Laboratory, 2015.

[10] J. Ortensi, A. Alberti, Y. Wang, M.D. DeHart, F.N. Gleicher, S. Schunert, and T.S. Palrmer. Methodologies and Requirements for the Generation of Physics Data Inputs to MAMMOTH Transient Simulations in Support of the Transient Reactor Test Facility. Technical Report NL/EXT-15-36265, Idaho National Laboratory, September 2015.

[11] T. H. Bauer W. R. Robinson. The M8 Power Calibration Experiment (M8CAL). Technical Report ANL-IFR-232, Argonne National Laboratory, May 1994.

[12] J. Leppänen. *Development of a New Monte Carlo Reactor Physics Code*. PhD thesis, Helsinki University of Technology, 2007.

[13] T. J. Trahan. *An Asymptotic, Homogenized, Anisotropic, Multigroup Diffusion Approximation to the Neutron Transport Equation*. Doctoral disseration, University of Michigan, Nuclear Engineering and Radiological Sciences Dept., 2014.

[14] J. Ortensi, S. Schunert, Y. Wang, B. A. Baker, F. N. Gleicher, M. D. DeHart. A Neutron Streaming Problem to Test Rattlesnake Methods for TREAT, INL/CON-16-39358. In *Proceedings of the ANS 2016 Winter Meeting*, Las Vegas, NV, Nov. 6-10 2016. American Nuclear Society (To be published).

[15] A. Hébert. Développement de la methode SPH: Homogénéisation de cellules dans un réseau non uniforme et calcul des paramètres de réflecteur. Technical Report CEA-N-2209, Commissariat à l'Energie Atomique, 1981.

[16] A. Laurier. *Implementation of the SPH Procedure within the MOOSE Finite Element Framework*. M.S. Thesis, École Polytechnique de Montréal, Montréal, Canada, 2016.

[17] J. Leppänen. Performance of Woodcock delta-tracking in lattice physics applications using the Serpent Monte Carlo reactor physics burnup calculation code, 2010.


INL
Idaho National Laboratory